Table 4.1. Bottom “roughness” final scheme used for classifying hydroacoustic and towed video.

Bottom roughness
Class 1 = low = soft sediments (sand, mud) with no or little bi-valve shell debris, rock, epibenthic organisms; vertical structure < 5 cm in most of area
Class 2 = low = mainly mud/sand mixtures with variable amounts of bi-valve shell debris, rock, epibenthos; vertical structure variable, < 10 cm in most of area
Class 3 = moderate = mainly packed shell debris and scattered rubble/rock with variable amounts of mud/sand mixtures, epibenthos variably abundant, vertical structure < 10 cm in most of area
Class 4 = high = intact bi-valve shells and hard bottom, mostly exposed bedrock, epibenthos typically abundant, vertical structure typically > 10 cm.
Class 5 = high = abundant drift macroalgae, or seagrasses, typically with attached macroalgae and other epibenthos, vertical structure > 10 cm

Table 4.2a-b. a), Comparison matrix of training dataset records classified by DA into 5 bottom roughness classes and by a PCA+K-means into five clusters; and b), the same data standardized to 100 cases per class (to remove bias of unequal sample sizes). Moving across rows note that 4 of the 5 K-Means Clusters were dominated by a single discriminant analysis (DA) Group, while the other was mostly Classes 3 and 4, validating the variance ratio criterion's (VRC) recommendation of 4 (or to a lesser extent 5) optimum classes.

a. Comparison Matrix of Training Dataset

K-Means	Exploratory DA 1	2	3	4	5	n
1	184	0	2	6	45	237
2	1372	71	102	36	0	1581
3	0	0	0	0	34	34
4	506	14	636	243	181	1580
5	76	1307	30	54	2	1469
n	2138	1392	770	339	262	4901

b. Standardized to 100 Cases per Class

K-Means	Exploratory DA 1	2	3	4	5	n	%
1	9	0	0	2	17	28	60.7
2	64	5	13	11	0	93	68.8
3	0	0	0	0	13	13	100
4	24	1	83	72	69	249	62.2
5	4	94	4	16	1	119	79.0
n	100	100	100	100	100	500	

Table 4.3. Confusion matrix of acoustically-predicted (MAP) versus ground-validated ("TRUTH") classifications of the 89 samples passing QA. Note: Class 5 was omitted as most of its samples were rejected by the minimum depth filter.

		TRUTH					
	Group	**1**	**2**	**3**	**4**	**row**	**User**
MAP	**1**	**28**	2			30	93.3
	2	5	**29**	3	1	38	76.3
	3		1	**5**		6	83.3
	4	1	5	0	**9**	15	60.0
	column	34	37	8	10	**89**	
	Producer	82.4	78.4	62.5	90.0	$P_o =$	**0.80**
						$T_e =$	**0.73**

Table 4.4. Video-based bottom classification scheme for estuarine and shallow Gulf of Mexico waters. Seven major classes (numbered 1 – 7 and enclosed by ellipses), each with two or more subclasses (a, b, c, etc.) are described in the here. The subclasses indicate: the dominant benthic organism (either: a, no benthos; b, sand dollars; and c, urchins, etc.).

	Dominant Sediment Type				
Dominant Benthos	**Sand**	**Shell/Sand**	**Low-relief Shell/Rock (=Reef)**	**High-relief Shell/Rock (=Reef)**	**Description by Major Class**
(None)	1a	2a			1 = Sand >90% with no or rare sessile epibenthos
Sand Dollars	1b	2b			2 = Shell/Sand mixtures with no or rare sessile epibenthos
Urchins	1c	2c	5c	6c	3 = Sand >90% with scattered to dense sessile epibenthos
Pen Shells	3d	4d			4 = Shell/Sand mixtures with scattered to dense sessile epibenthos
Soft Corals	3e	4e	5e	6e	5 = Low-relief (<20 cm height) hard bottom with diverse benthos
Hard Corals			5f	6f	6 = High-relief (>20 cm height) hard bottom with diverse benthos
Sponges		4g	5g	6g	7 = Sand >90% with macroalgae and/or seagrasses
Macroalgae	7h	4h	5h	6h	NOTE: All classes except Class 1 (Sand with no or mainly motile benthos) are bottom types with potential for macroalgae attachment
Seagrasses	7i	4i			

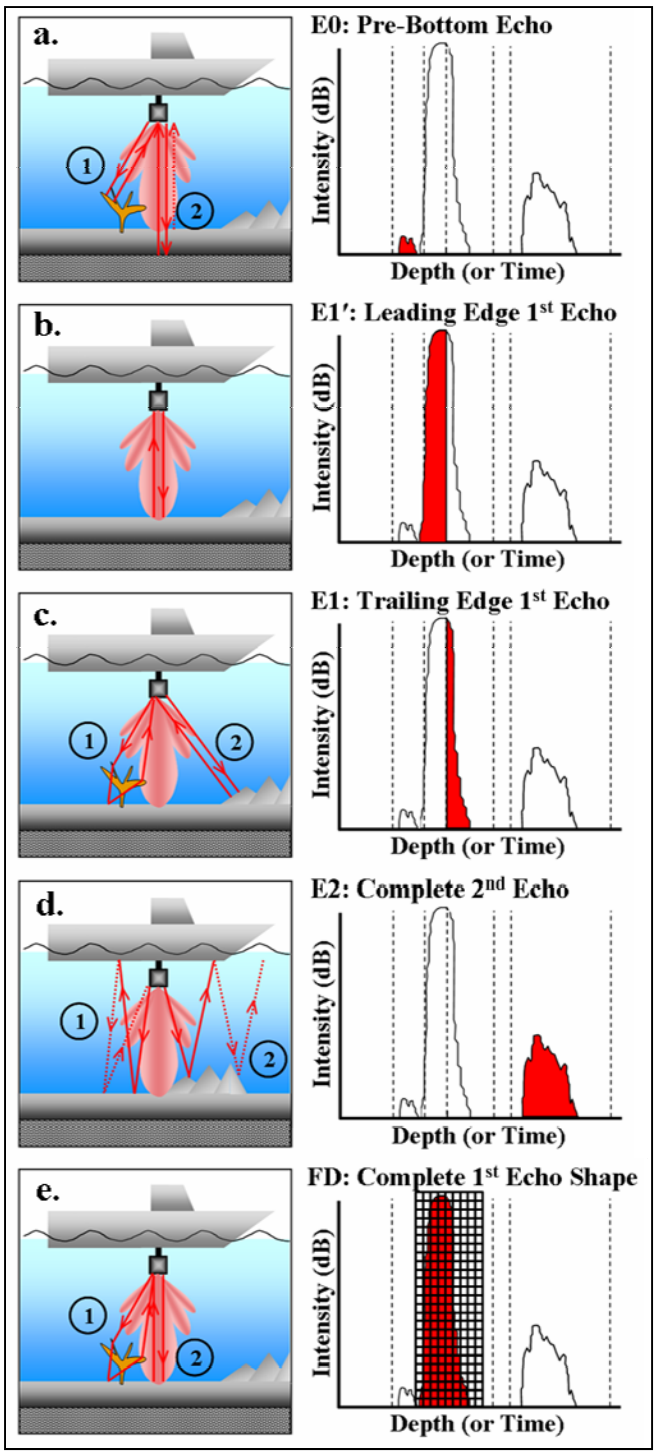

Figure 4.1. Acoustic energy (E0, E1’, E1, E2) and shape (FD) parameters computed from single-beam ASC echo envelopes.

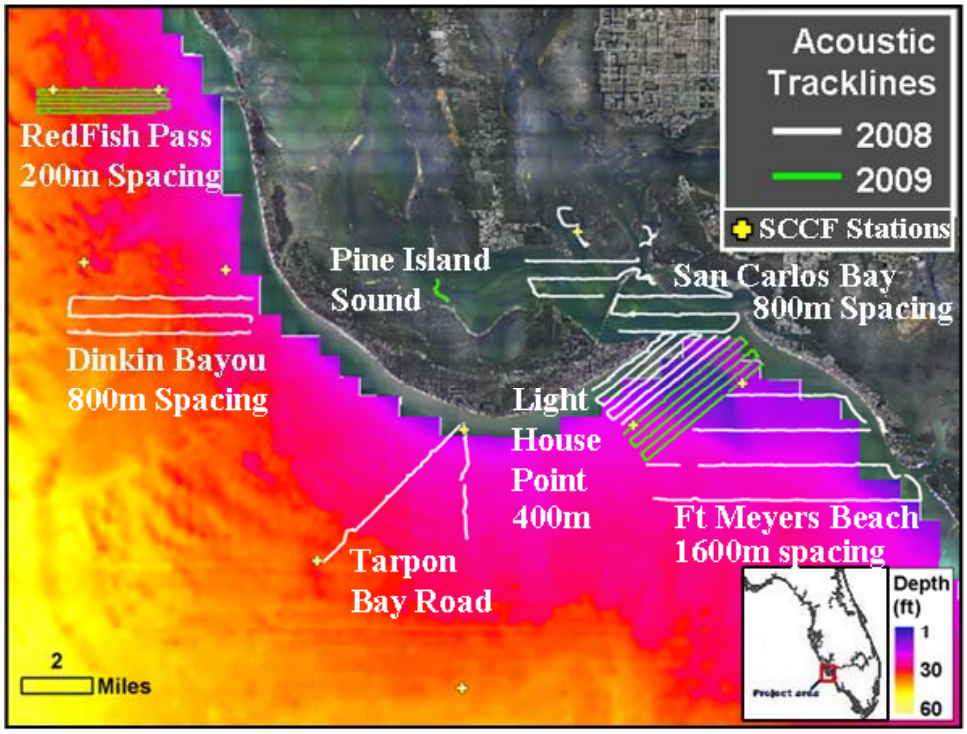

Figure 4.2. GPS trackplots of hydroacoustic surveys, conducted during the periods of October 2008 and May 2009. Yellow crosses (+) denote the location of sampling stations for Objective 5, Sanibel-Captiva Conservation Foundation Marine Laboratory.

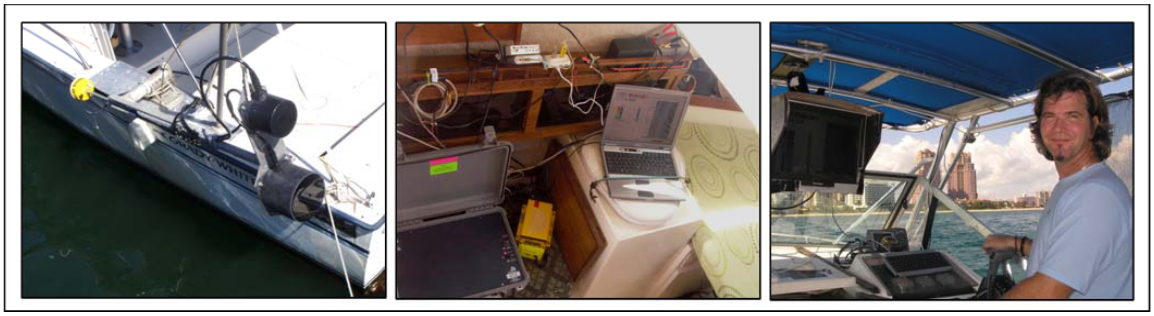

Figure 4.3. Hydroacoustic survey equipment. Left image, swing-arm in horizontal (traveling) position with 420 and 38 kHz transducers and Trimble antenna. Middle image, inside v-berth of survey vessel with BioSonics DT-X echosounder, Trimble receiver, and acquisition PC. Right image, monitor displaying GPS-navigation over pre-planned lines and real-time echo returns.

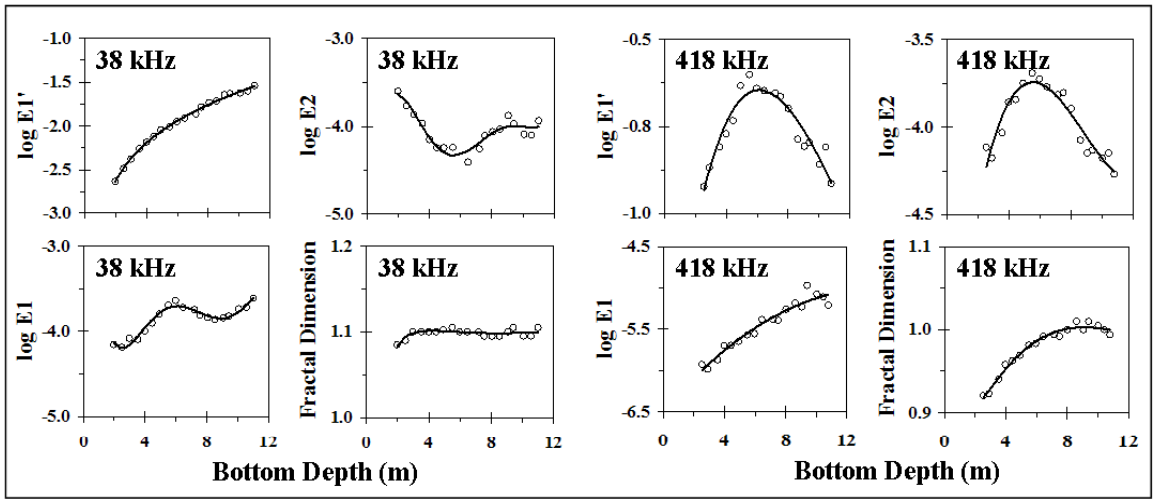

Figure 4.4. High-order logarithmic polynomials (solid lines) were fit to the median values of acoustic parameters at 18 bins of depth (○) used to normalize acoustic parameters to median survey depth.

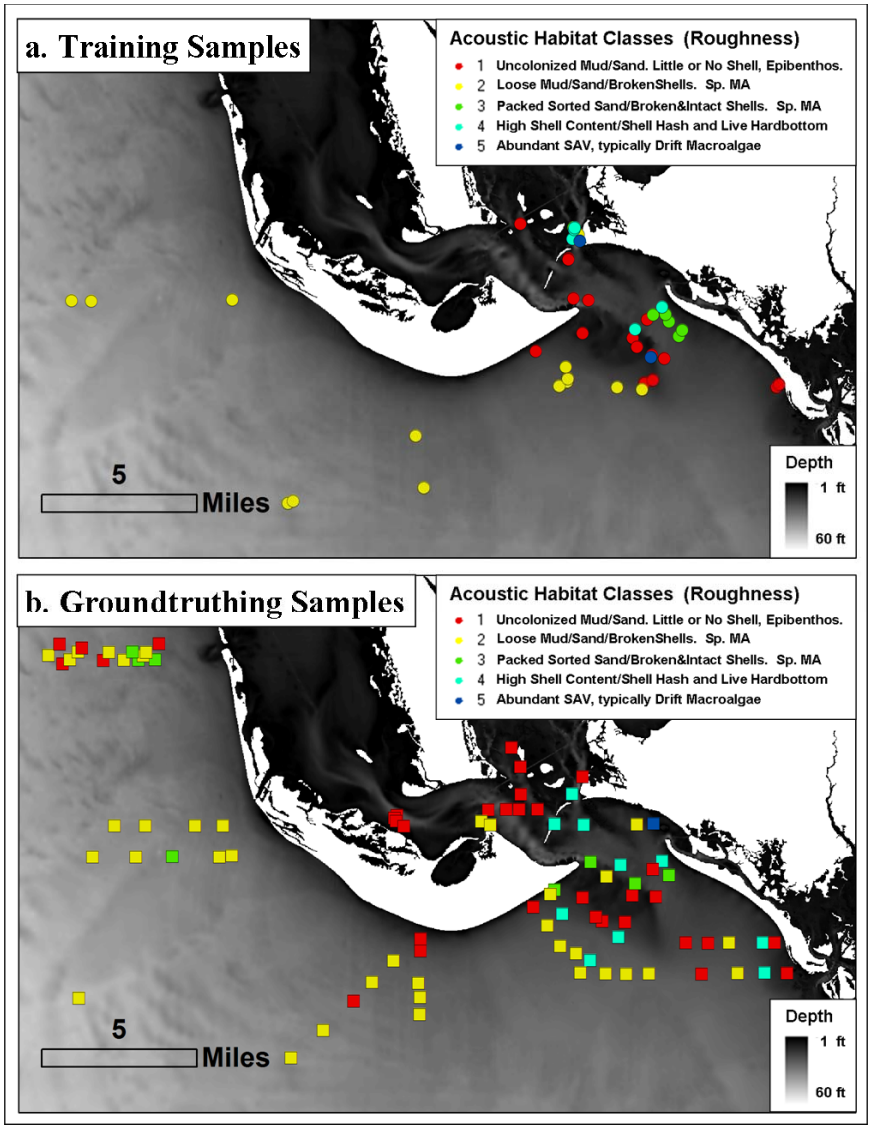

Figure 4.5. Locations of: a), training; and b), accuracy assessment samples. Each sample consisted of a discrete sonar file and a spatially-coincident video file.

Class 1. uncolonized mud/sand, little or no shell, epibenthos

Class 2. mud/sand with variably sparse shell, rock epibenthos

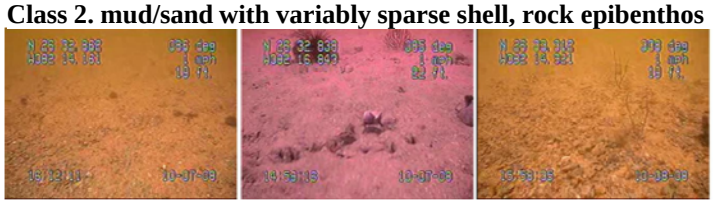

Class 3. packed/sorted sand/shells, sparse MA.

Class 4. high shell content, shell hash and live hard bottom

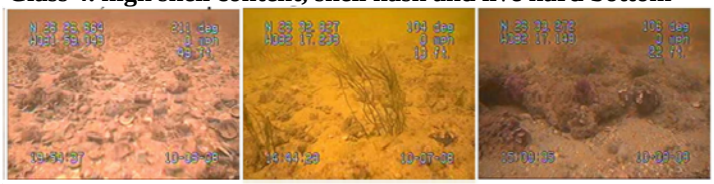

Class 5. abundant SAV

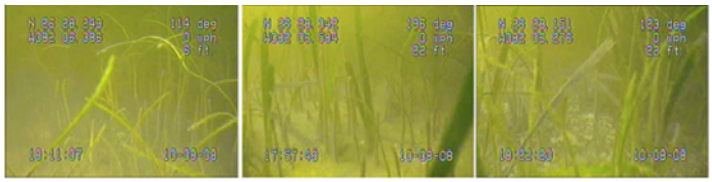

Figure 4.6. Screen captured stills taken from ground-validation videos, representing typical substrate and biota of the five acoustically-derived, Seabed Classes used for supervised classification of Phase I and II mapping.

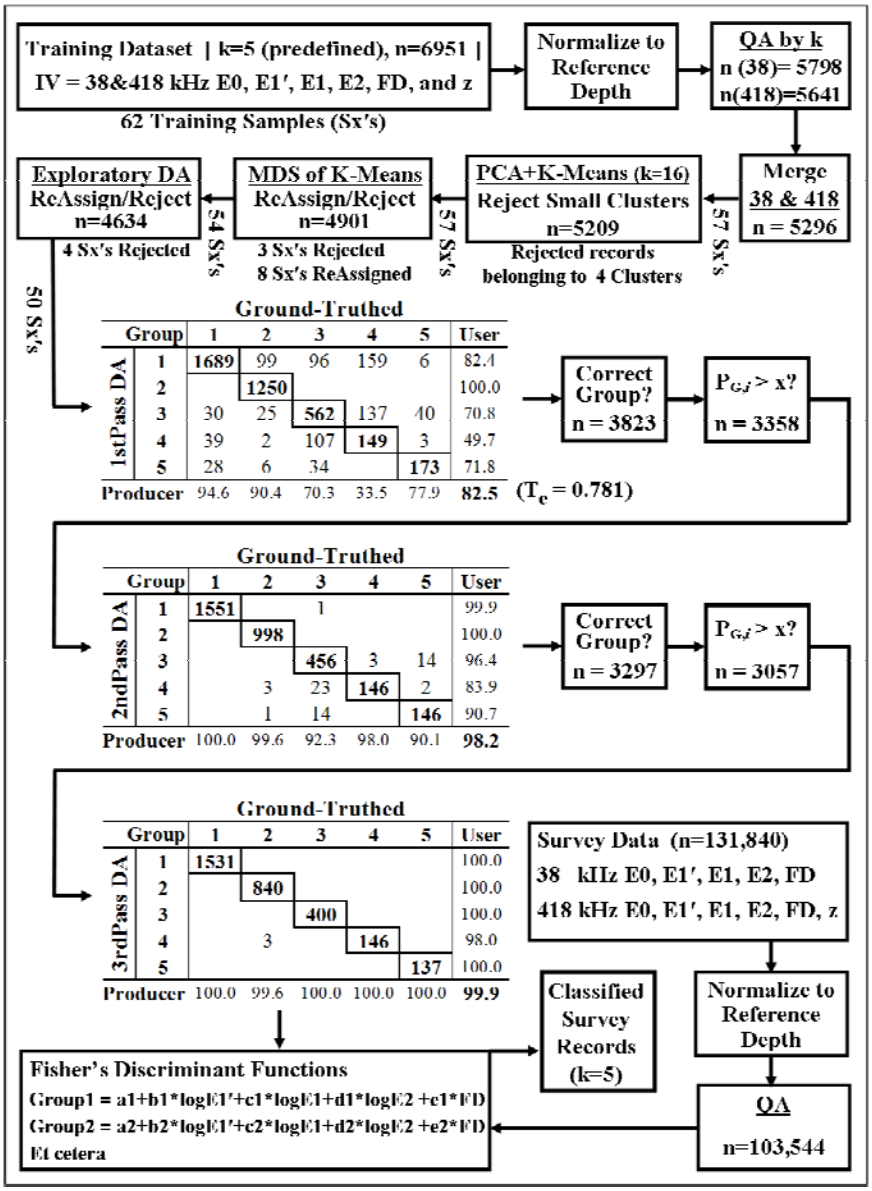

Figure 4.7. Classification workflow for classification. Hydroacoustic training samples were assigned to one of five *a priori* bottom classes. Acoustic parameters were normalized to average survey depth, using empirical models created from survey and select training data. Quality analysis consisted of a max depth span, min/max depth, and 1 of 99 percentile filters (calculated individually for each training group), followed by PCA/K-means/MDS outlier filtering and class re-assignment. The final membership of training dataset was determined using an exploratory discriminant analysis (DA). The training dataset was refined by passing through three DAs. Only those training records: (1) classifying correctly; and (2) exceeding a minimum probability for group membership passed onto the next DA. The Fisher's Linear Discriminant Functions obtained from the 3rd DA were used to classify survey data into one of five final *a priori* bottom classes.

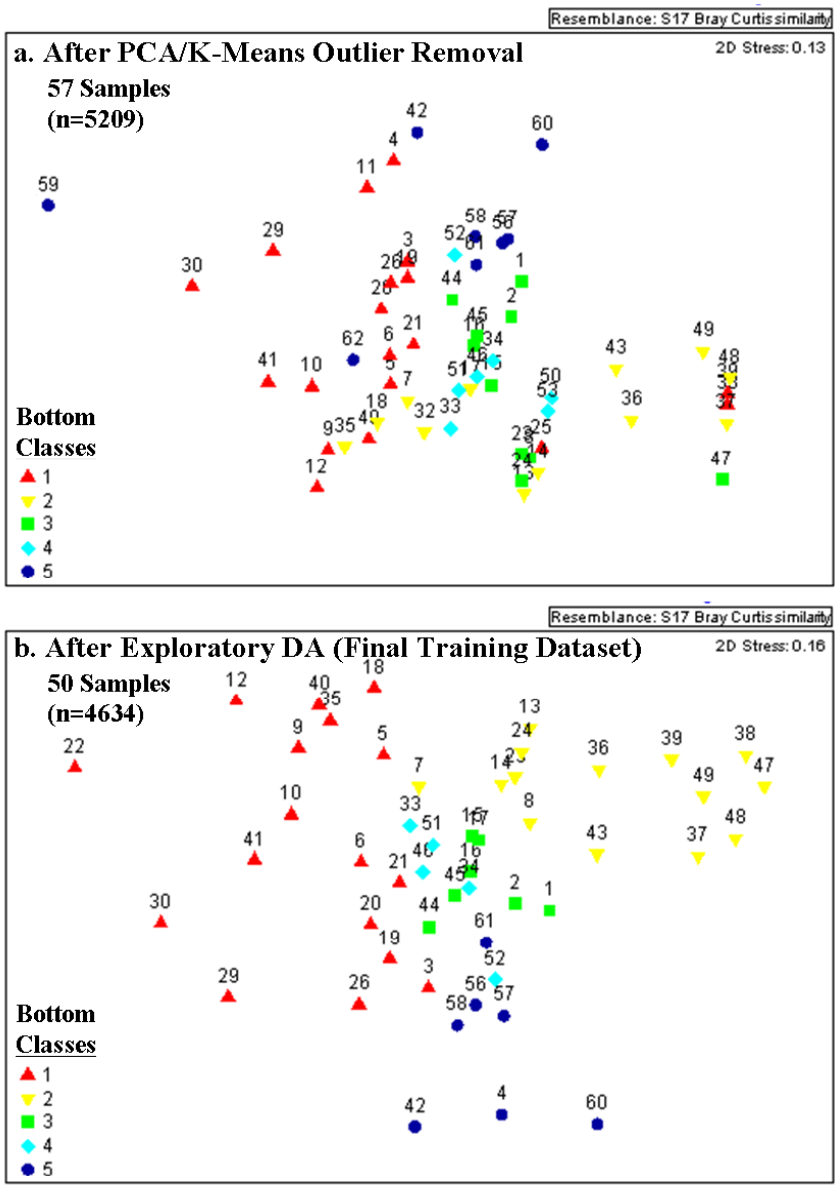

Figure 4.8. 2-D MDS plots of training dataset constructed from Bray-Curtis similarity matrix after: (a) rejecting four disproportionately small PCA+K-means clusters; and after (b) final rejection/reassignment of training records/samples following the exploratory Discriminant Analysis (DA).

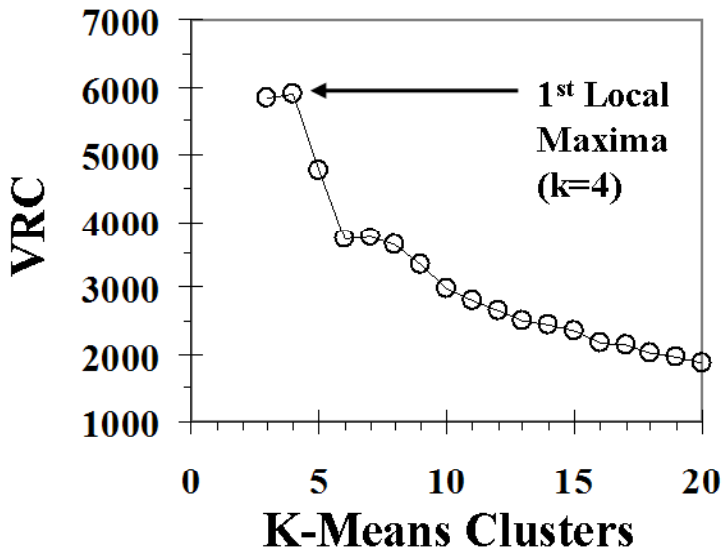

Figure 4.9. Variance ratio criterion (VRC) suggested an “optimal” number at four total bottom classes.

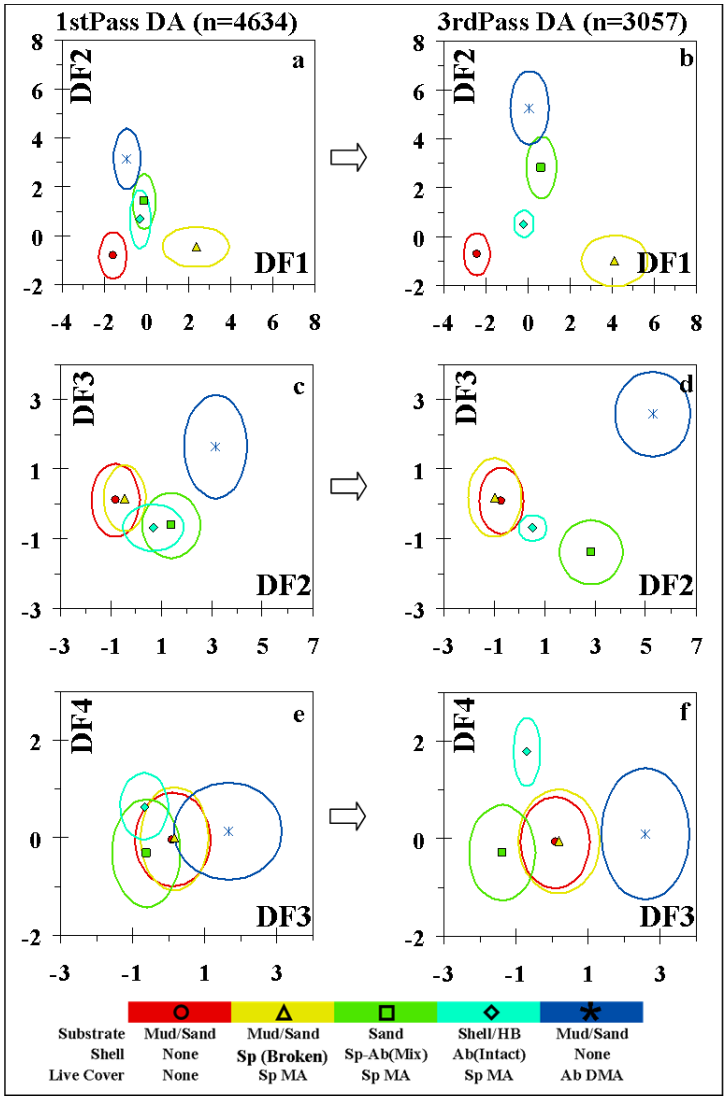

Figure 4.10. Plots of Discriminant Functions from the supervised classification of the training dataset into five discrete bottom classes by multipass Discriminant Analysis (DA). Center points denote cluster averages, ellipses are dispersion (1SD) about an X and Y. Left three graphs are from data submitted to the 1st Descriptive DA. Right three graphs are the results of the 3rd pass descriptive DA. Note the resulting refinement of the training dataset as shown by a greater separation between groupings.

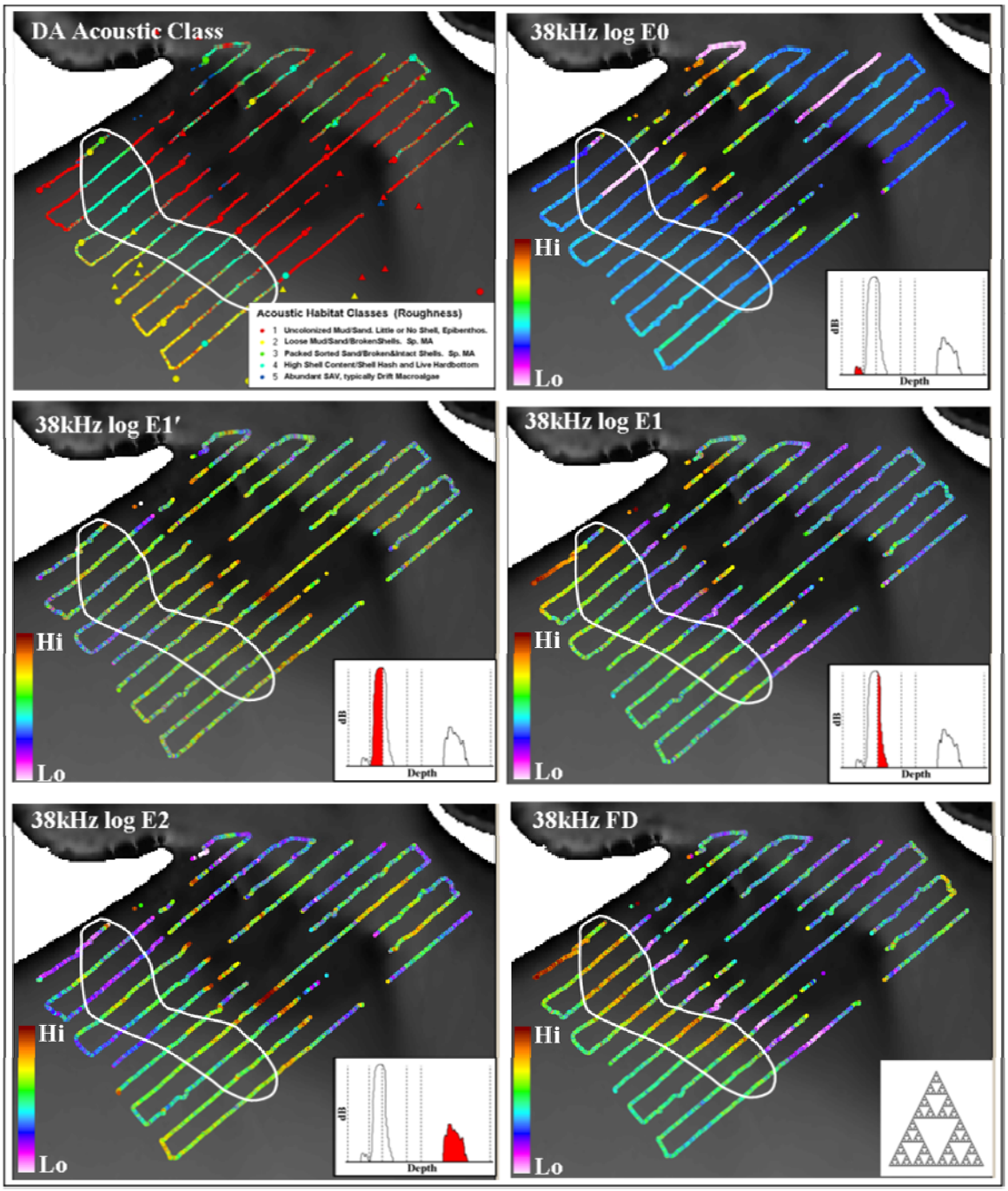

Figure 4.11. Classified acoustic GPS trackplot (see upper left) and trackplots of 38 kHz acoustic energy parameters and fractal dimension (E0, E1, E1', E2, FD) for Lighthouse Point. The boundary of the acoustically-"rough" bottom is indicated for reference.

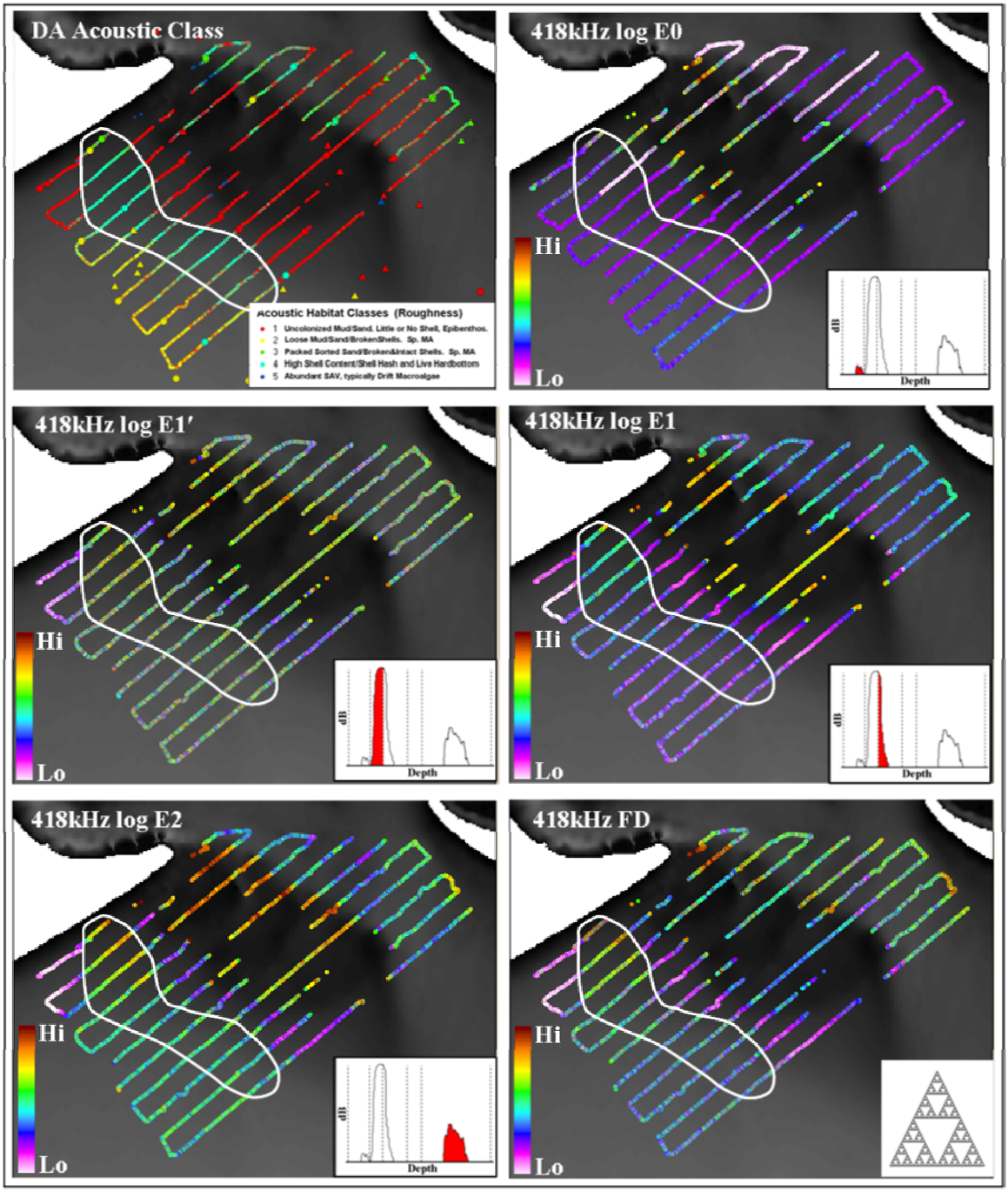

Figure 4.12. Classified acoustic (see upper left) and GPS trackplots of 418 kHz acoustic energy parameters and fractal dimension (E0, E1, E1', E2, FD) for Lighthouse Point. The boundary of the acoustically-"rough" bottom is indicated for reference.

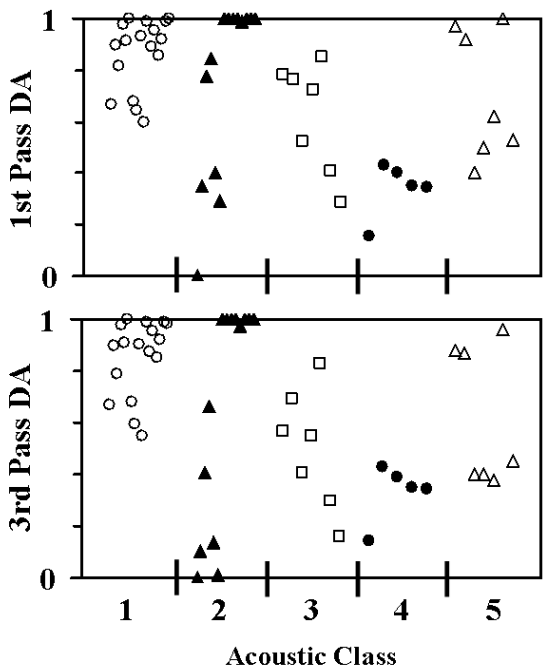

Figure 4.13. Equitable rejection of records among individual training samples suggest suggests the independent variables represented spatially and temporally consistent seabed characteristics of the five acoustic classes (each symbol represents one of the 50 catalog samples comprising the five class training dataset). Proportion of training dataset records that: (1) classified correctly; and (2) exceeded the minimum probability of group membership following the 1st (upper) and 3rd (lower) Descriptive DA.

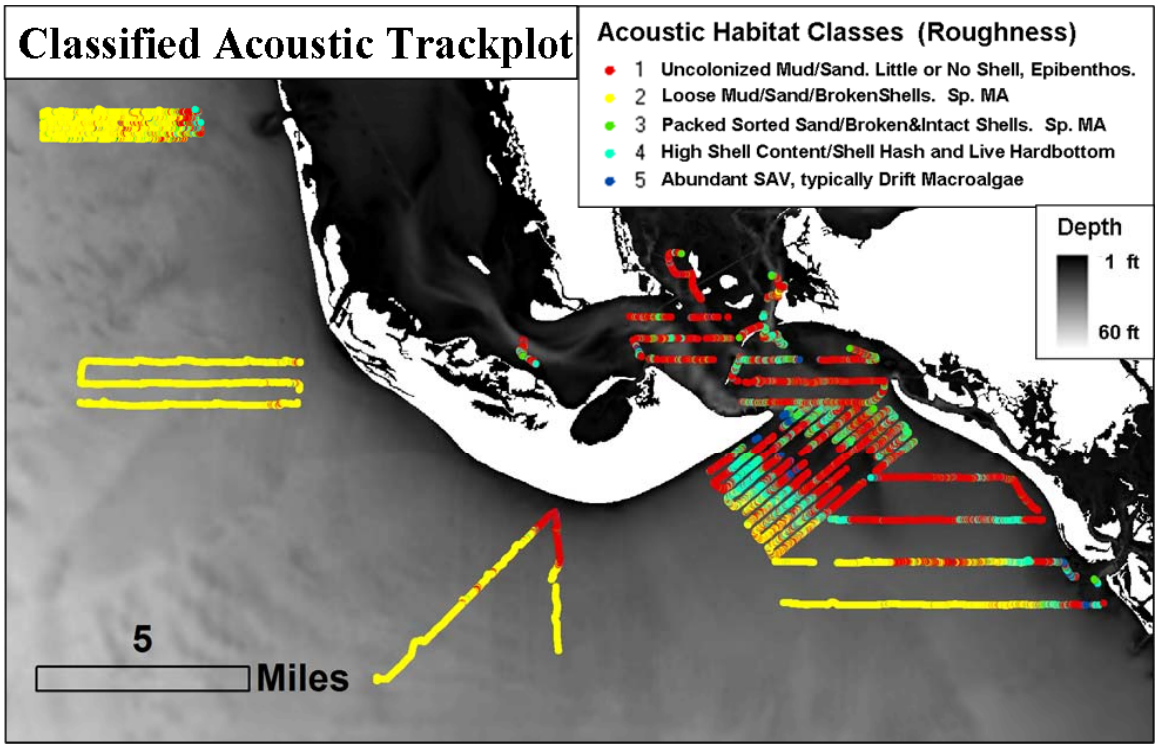

Figure 4.14. Classified GPS trackplot of 2008-09 hydroacoustic surveys, using the Fisher's Linear Discriminant functions obtained from the 3rd Pass Descriptive DA.

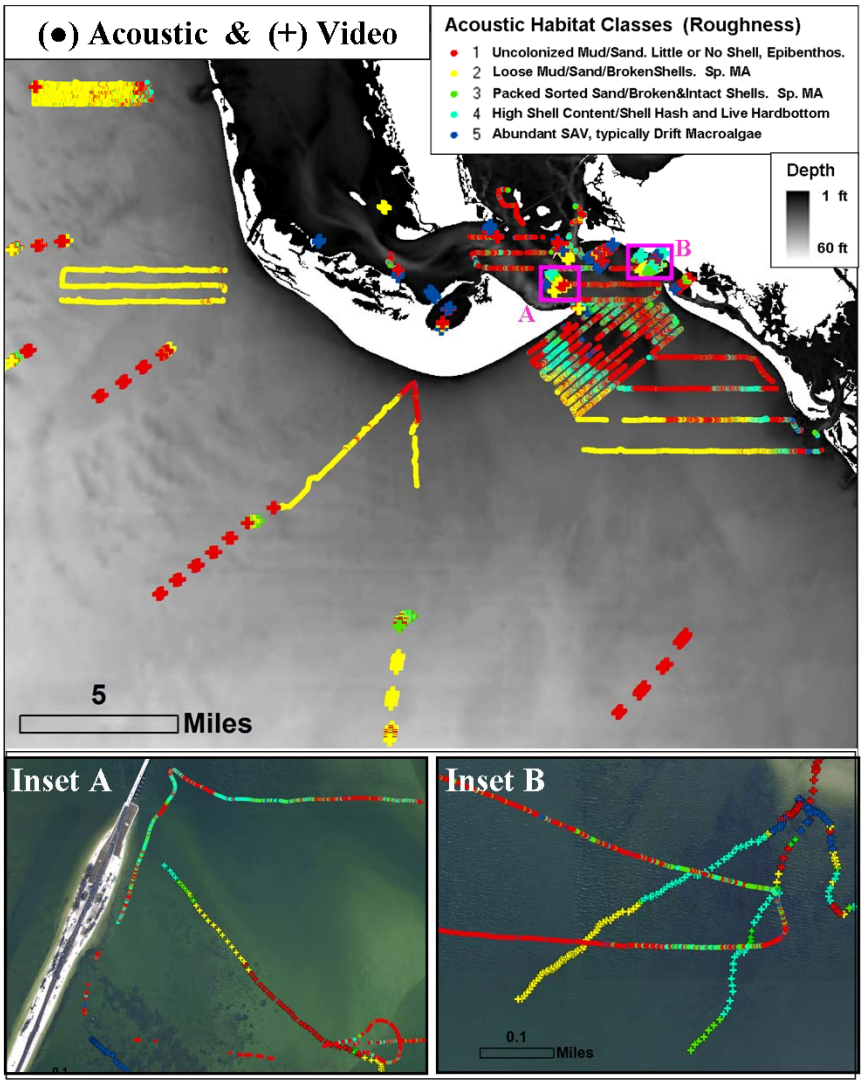

Figure 4.15. Classified hydroacoustic GPS trackplots and classified towed-video transects. Note for Insets A and B (blow-up below), areas where hydroacoustic and towed-video transects intersected the two methods closely agreed on classifications.

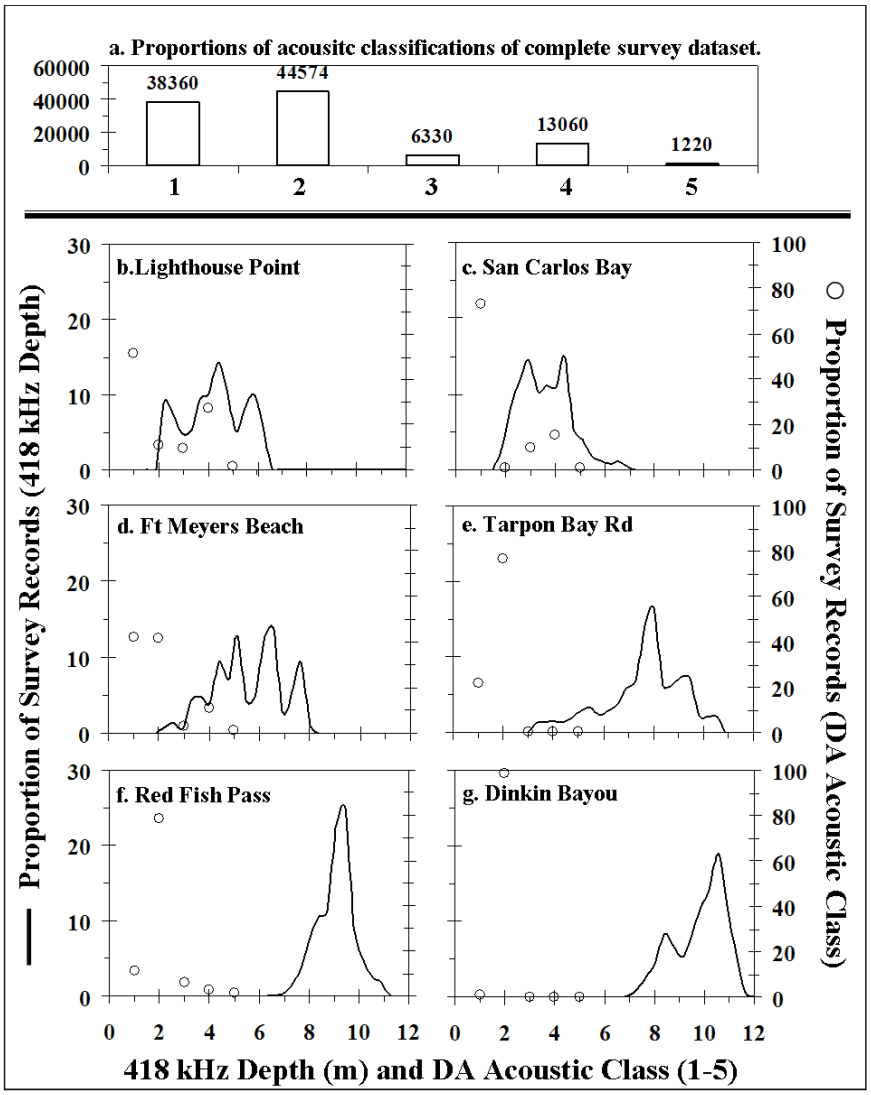

Figure 4.16. Bathymetric and acoustic class profiles of specific survey sites. Top:, a), distribution of hydroacoustic survey records for the five acoustic bottom classes for the complete overall survey; and lower, b-g) histograms for the 418 kHz bottom depth (solid line) and distribution of survey records among the five bottom classes (○) for each survey site.

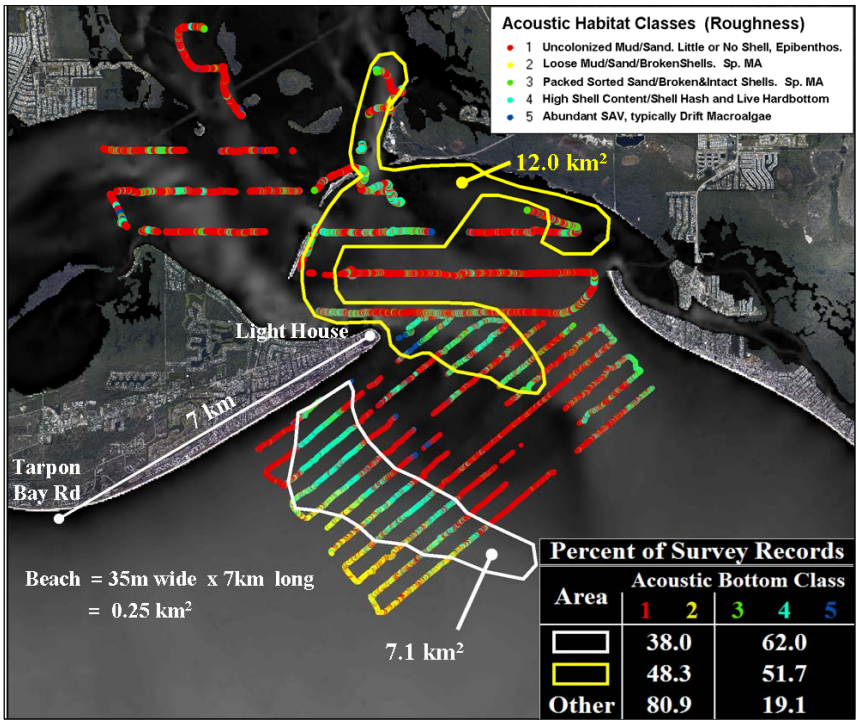

Figure 4.17. Assessment of the potential for Lighthouse and San Carlos Bay sites to generate nuisance macroalgal blooms. Classified hydroacoustic GPS trackplots of the San Carlos Bay and Lighthouse Point surveys. Demarcations denote areas of high acoustic "roughness" (i.e. high proportion of Bottom Classes 3, 4 and 5). Inset (bottom-right) shows the distribution of hydroacoustic survey records among the five Bottom Classes within the two "rough" areas as compared to the other records lying outside of the "rough" demarcations.

	Dominant Sediment Type			
Dominant Benthos	**Sand**	**Sand/Shell**	**Low-relief Shell/Rock (=Reef)**	**High-relief Shell/Rock (=Reef)**
(None)				
Sand Dollars				
Urchins		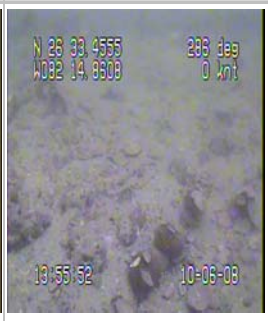	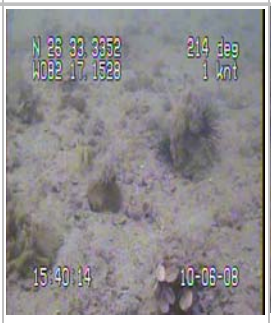	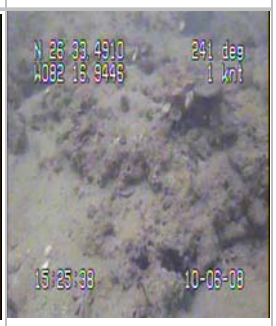
Pen Shells		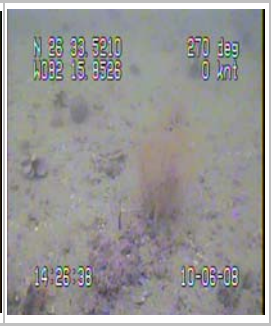		

Figure 4.18. Video still (captured) images illustrating the various Classes and Subclasses for the video-derived seabed classification scheme used in Table 4.4.

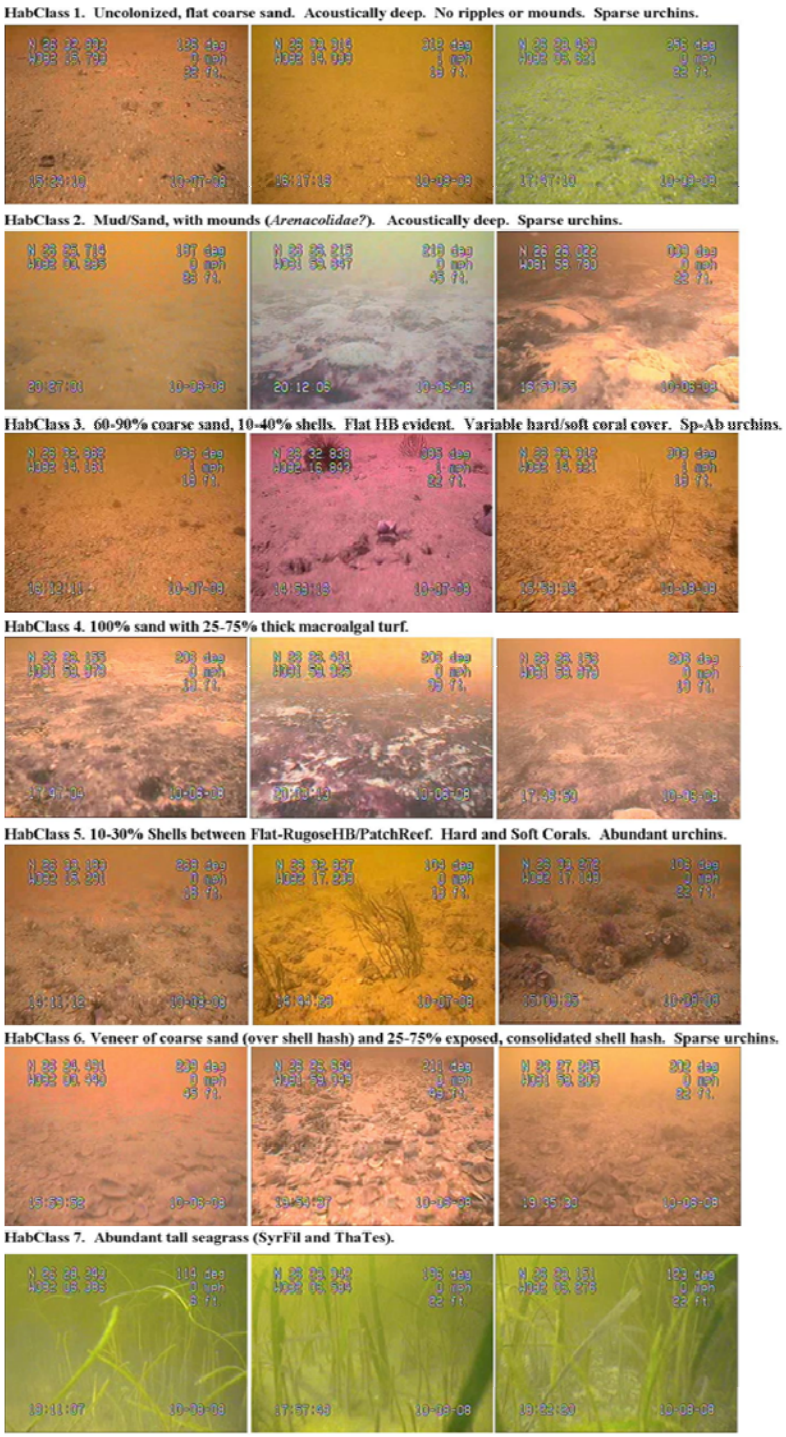

Figure 4.19. Captured stills taken from ground-validation videos, representing typical substrate and biota of the seven acoustically-derived Seabed Classes obtained from the unsupervised classification of the Phase I hydroacoustic data. The seven overall derived-classes were consolidated into five Classes for the final supervised classification of hydroacoustic data from Phases I and II (see Figure 4.6 also).

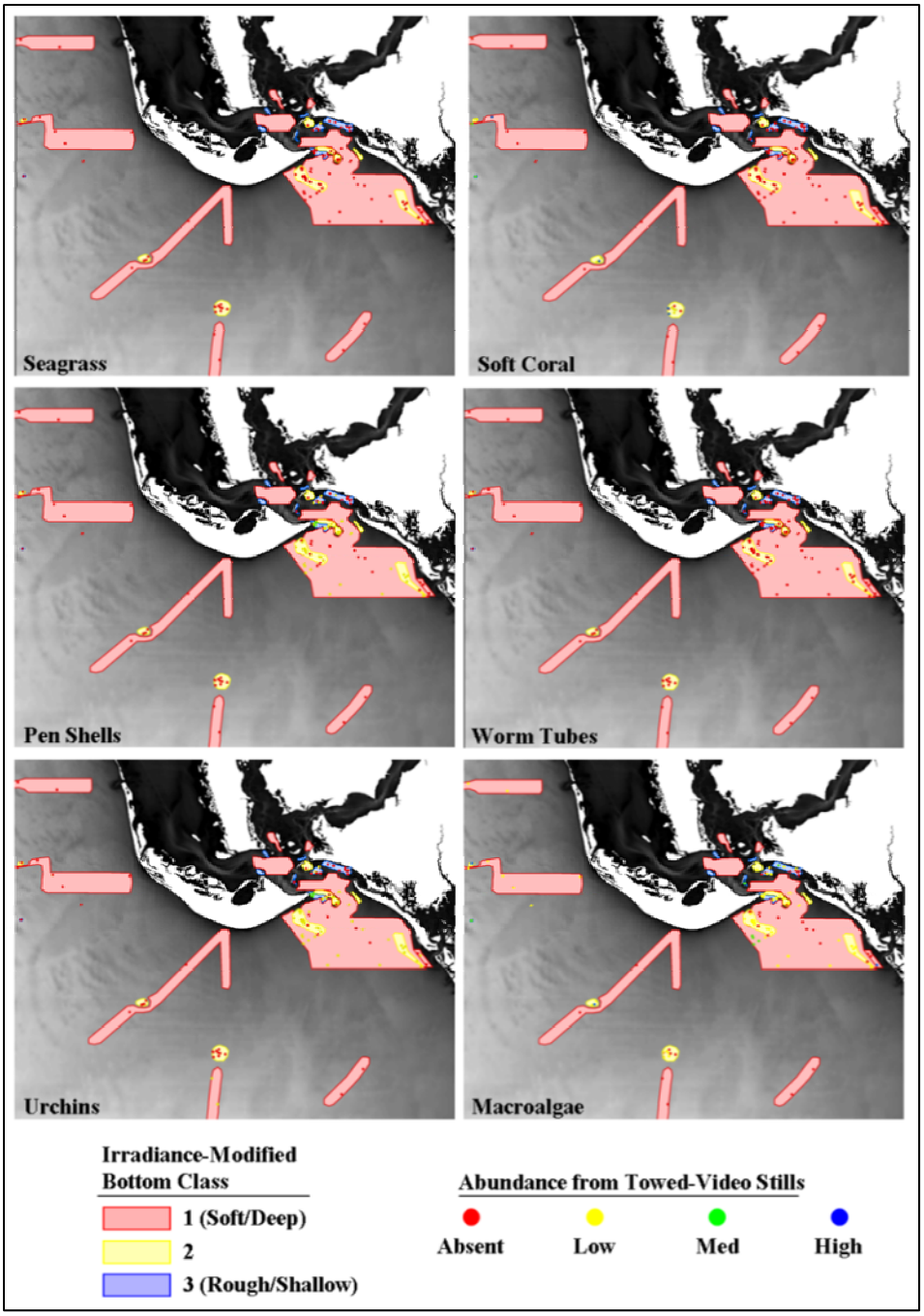

Figure 4.20. 'Expert' classification of biogenic features from stills of Phase III towed-video, displayed over irradiance-modified acoustic bottom class.